

250 nm Glycine-Rich Nanodroplets Are Formed on Dissolution of Glycine Crystals But Are Too Small To Provide Productive Nucleation Sites

Anna Jawor-Baczynska,[†] Jan Sefcik,[†] and Barry D. Moore^{*,‡}

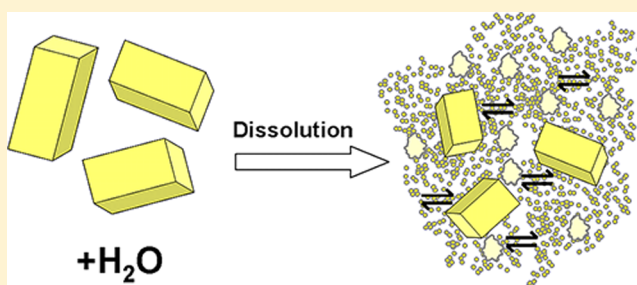
[†]Department of Chemical and Process Engineering, University of Strathclyde, 75 Montrose Street, Glasgow G1 1XJ, United Kingdom

[‡]WestCHEM, Department of Pure and Applied Chemistry, University of Strathclyde, 295 Cathedral Street, Glasgow G1 1XL, United Kingdom

S Supporting Information

ABSTRACT: Recent theoretical and experimental studies have proposed a two-step mechanism for crystal formation in which crystal nucleation is preceded by formation of disordered molecular assemblies. Here, we investigated whether similar intermediates might also form as crystals dissolve, effectively the reverse process. A model system of glycine in water was studied, and the resultant solutions were characterized using small-angle X-ray scattering, dynamic light scattering, and nanoparticle tracking analysis. Invariably, dissolution of glycine crystals into water was observed to produce scattering nanospecies with liquid-like properties and a mean diameter of about 250 nm, at near saturation concentration.

The nanospecies persisted indefinitely in solution in the presence of excess glycine crystals and were identified as glycine-rich nanodroplets with an equilibrium population of about 10^9 per mL. The time to appearance of glycine crystals from quiescent supersaturated solution ($S = 1.1$) containing either a low population of nanodroplets (nanofiltered) or a high population of nanodroplets (unfiltered) was indistinguishable with typically only a single crystal forming after about 30 h. However, a very significant acceleration of crystal formation was observed whenever a gently tumbling stirrer-bar was introduced into the vial; thousands of microcrystals appeared after an incubation period of only 3–5 h. The possibility of this being caused by factors such as secondary nucleation, bubbles, or glass splinters or scratches was eliminated via control experiments. Further investigation of the glycine solution, just prior to appearance of microcrystals, revealed an additional subpopulation of extremely large glycine-rich nanodroplets (diameter >750 nm), not observed in quiescent solutions. It is proposed that productive nucleation of glycine crystals occurs exclusively within these larger glycine-rich nanodroplets because a critical mass of glycine is required to form nascent crystals large enough to survive exposure to bulk more dilute solution. We hypothesize that nucleation occurs frequently but nonproductively within subcritical mass nanodroplets and infrequently but productively within very rare critical mass solute-rich nanodroplets. Such a model provides a new compelling way of bridging classical mechanisms of crystal nucleation with the more recently proposed two-step processes.



INTRODUCTION

Understanding of the mechanism of nucleation of crystals from solution is crucial for many natural and industrial processes, from biomineralization of bones and teeth to production of pharmaceuticals and nanomaterials. The most generally accepted mechanism is that nucleation from supersaturated molecular solutions occurs via transient assembly and organization of molecules to produce nascent nuclei, and very occasionally these attain a critical size and continue to grow into macroscopic crystals. Many studies have therefore attempted to probe molecular self-organization in solutions and melts with the aim of identifying a relationship between the structure of nascent nuclei and the resultant crystal polymorphs formed.^{1–4} Commonly, in supersaturated solutions, small molecular clusters of solute are experimentally observed,^{1–6} but correlation with molecular organization in the crystal has

been difficult to achieve. Larger nanoclusters, with liquid-like properties, have been reported in concentrated protein solutions^{7–10} and glycine aqueous solutions⁵ and implicated as possible metastable intermediates on the crystallization pathway. These results, combined with theoretical studies, led to the proposal of an alternate two-step process of crystallization^{11–13} in which disordered metastable molecular assemblies, containing relatively large numbers of solute (and solvent) molecules, are produced prior to the nucleation of more ordered nascent crystals. Interestingly, a crystallization pathway involving nanoscale intermediates has also been reported for mesostructured crystals in which nanoparticles

Received: February 1, 2012

Revised: November 11, 2012

Published: December 6, 2012

initially form a crystal-like lattice that subsequently transforms into a single molecular crystal.^{11,14–17}

In this study, we decided to investigate whether the disordered molecular assemblies proposed as intermediates in the two-step model could also be produced by a reverse process, involving (partial) dissolution of crystals. It was noted that most studies of crystal nucleation had previously focused on trying to identify and characterize molecular assemblies made up of a relatively small number of molecules (2–100) and had therefore used techniques sensitive to short length-scales (<1 nm). In this work, we used both X-ray scattering and light scattering techniques, to provide sensitivity to assemblies over a much greater range of length-scales. In particular, these methods were used to probe for any scattering particles produced during the dissolution of crystals of the small amino acid, glycine, into aqueous solution. Uniquely, some of these scattering experiments were carried out under equilibrium conditions, in which the crystalline glycine phase was continuously present. This allowed the possibility of distinguishing between metastable entities and those in thermodynamic equilibrium. The results suggest glycine-rich nanodroplets of around 250 nm diameter form as solid glycine dissolves in water and coexist in equilibrium with glycine crystals. These species appeared to not be directly involved in productive crystal nucleation (from weakly supersaturated solutions) but could be coalesced to provide access to a much more rapid nucleation pathway.

■ EXPERIMENTAL SECTION

Solutions of glycine with concentration 270 mg/mL of water (supersaturated at 25 °C) were prepared by combining solid glycine ($\geq 99\%$ NT from Fluka) and deionized water (from an in-house Millipore Water System, 18 M Ω /cm) in glass vials sealed with a screw-on cap. The glycine was completely dissolved by stirring at 55 °C (in an incubator) typically for at least 24h. Because studies using scattering techniques are extremely sensitive to experimental artifacts, very great care was taken to avoid introduction of adventitious species. Prior to analysis (DLS, NTA, SAXS), the samples were filtered at 55 °C using either 100 nm PTFE or 20 nm Anotop filters, and control water samples were also run. All syringes, filters, cuvettes, and tubes were preheated in an incubator at 55 °C to avoid premature cooling of the solution during filtering and transfers. NTA and DLS sample cells were preheated to 50 °C before the solution was introduced and then cooled and equilibrated at 25 °C for 5 min prior to the start of data collection. Crystallization experiments were carried out in glass HPLC vials (volume 1.5 mL from Chromacol) with or without a PTFE-coated magnetic stirrer bar (12 mm \times 4.5 mm; with octagonal ring around axis) at constant temperature 25 °C. Reported crystallization experiments were repeated at least 75 times. Where described, continuous inversion of the vials (tumbling) was carried out using a blood tube rotator (SB2 Stuart with constant speed 20 rpm and fixed mixing angle 65°, tube holder SB3/1).

The filters used in the study were Puradisc 13 syringe filters, 0.1 μ m, PTFE Whatman, cat. no. 6784-1301 (“100 nm PTFE”) and Inorganic membrane filters Anotop 10 Syringe Filters, 0.02 and 0.1 μ m Whatman, cat. nos. 6809-1002 and 6809-1012 (“20 nm Anotop” and “100 nm Anotop”, respectively). The practical performance of these filters was assessed using standard solid polystyrene latex microspheres 100 and 200 nm from ThermoScientific (3000 Series Nanosphere Size Standards).

Dynamic Light Scattering (DLS) Measurements. DLS measurements were carried out using an ALV/LSE- 5004 instrument, equipped with temperature control, using at a scattering angle $\theta = 90^\circ$ and laser light wavelength $\lambda = 632.8$ nm. DLS is a well-established experimental technique for studying nanoscale species in dispersions. By measuring the time-dependent fluctuations of scattered light

intensity, arising from Brownian motion, average diffusion coefficients and corresponding mean hydrodynamic diameters can be inferred. From the analysis of a measured autocorrelation function, the intensity averaged mean hydrodynamic diameter of nanospecies was estimated using the cumulant method¹⁸ (see the Supporting Information).

Nanoparticle Tracking Analysis (Brownian Microscopy). Nanodroplet size distribution and estimated concentrations were determined with a Nanosight LM10 instrument with temperature control unit. Nanosight NTA2.1 software was used to analyze videos and calculate the size and concentration of nanodroplets. The camera of the instrument was set using the “Autosettings” option to allow the software to optimize the shutter and gain settings. The sample was introduced into the viewing unit, and images of the species of the laser light were captured by a CCD camera attached to a microscope. A video of the sample was recorded and processed, with each observed individual species “tracked” by the nanoparticle tracking analysis (NTA) software. Each video was recorded for 90 s, and the processing parameters of brightness and gain were optimized by the software. From the Brownian motion analysis, the corresponding diffusion coefficient was calculated from the mean squared displacement of the species tracked and substituted into the Stokes–Einstein equation to obtain the species hydrodynamic diameter. Estimation of the species concentration was based on the species count in the illuminated volume calculated from the dimensions of the field of view (at a given magnification) and the dimension of the laser beam. The particle concentration measurements are subject to a variation of up to 25% between identical samples.

Small-Angle X-ray Scattering (SAXS) Measurements. Small-angle X-ray scattering measurements were carried out at the SWING beamline at the SOLEIL synchrotron source in Gif-sur-Yvette, France. Aqueous solutions of glycine (270 mg/mL of water), prepared at 55 °C, were injected into a thermostatted automatic sample changer and cooled and equilibrated for 5 min at 25 °C. The sample was then automatically passed through a thermostatted capillary for exposure to X-ray radiation and detecting of scattered intensity patterns. The beam energy was 8 keV and sample–detector distance was 2.227 m, accessing a Q value range between 0.001 and 0.17 \AA^{-1} . Five measurements were recorded with an exposure time of 1 s each and 2 s delay time, checked for repeatability and averaged. The PCCD 170170 (AVIEX) 2D-detector was in the vacuum chamber equipped with a pumping system to achieve a primary vacuum of 10^{-6} bar to enable lower angles to be reached and avoid scattering from air molecules. The same measurement procedure was used for water samples. The integration and processing of the scattering data was carried out by using the software provided at the beamline.

■ RESULTS

This section initially describes results from a series of linked experiments in which three different scattering techniques were used to study the nanospecies formed on dissolution of glycine in water. Subsequently, the potential role played by these nanospecies in the nucleation of glycine crystals was investigated.

Observation of Nanospecies on Dissolution of Glycine in Water. The dissolution of glycine crystals in pure water to a concentration of 270 mg/mL was carried out at 55 °C, and this solution remained optically clear on cooling to 25 °C. However, on analyses using small-angle X-ray scattering (SAXS), nanoparticle tracking analysis (NTA), and dynamic light scattering (DLS), it was observed that a small population of nanoscale scattering species with a median diameter of around 250 nm was present. The glycine solution passes from an under-saturated state to a supersaturated state over the temperature range from 55 to 25 °C, but interestingly nanospecies were detected throughout. An estimate of the concentration of nanospecies at 25 °C was obtained from NTA giving a total population of around 10^9 per mL. Multiple

recrystallizations of the glycine from a range of solvents had no effect on the size or number of nanospecies produced, and attempts to generate similar species in pure water using a variety of stirring and heating protocols were unsuccessful.

Figure 1a,b shows the distribution of hydrodynamic diameters of nanoscale species in a supersaturated glycine

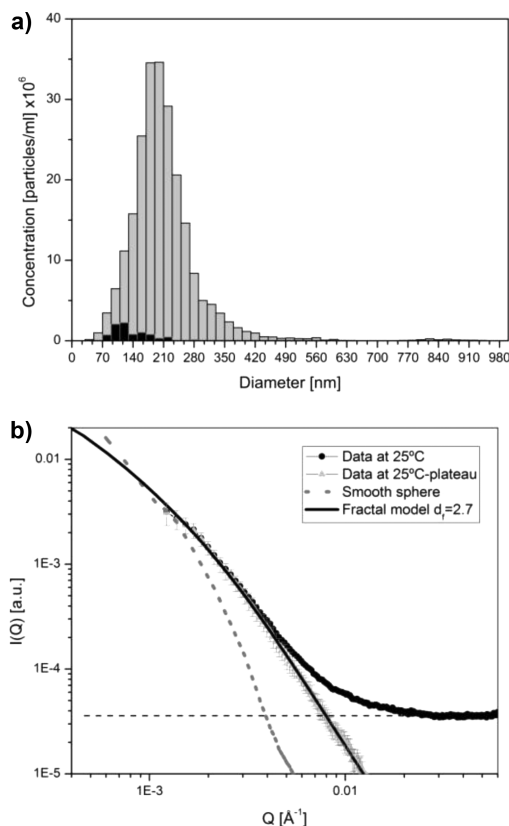


Figure 1. (a) Hydrodynamic diameter distribution (from NTA) of nanospecies at 25 °C, 270 mg/mL glycine aqueous solution filtered using 100 nm PTFE filter (gray bars) and blank water filtered using 100 nm PTFE filter (black bars). (b) SAXS experimental data (●) for the same solution and net scattering from nanospecies after subtraction of high Q plateau (gray ▲) plotted with best fits using smooth sphere model (gray ---) and mass fractal model (—) with fractal dimension $d_f = 2.7$.

solution at 25 °C (270 mg/mL water, relative supersaturation $S = 1.1$) determined by NTA and the measured SAXS intensity at low Q values for the same solution. By using the experimentally measured nanospecies size distribution from NTA, the SAXS intensity corresponding to various structural models was calculated for the entire ensemble of nanospecies.

We show in Figure 1b the calculated scattering intensities for both a smooth sphere model and a mass fractal model. The smooth sphere model does not have any adjustable parameters and gave a poor fit to the SAXS data because the slope in the power law region was much less than -4 expected for smooth nanospheres. This indicates the observed nanospecies do not possess a sharp interface as would be expected if they were nanobubbles or smooth spherical droplets. On the other hand, an excellent fit was obtained using a fractal model with the fractal dimension $d_f = 2.7$ (confidence interval ± 0.1). This suggests a population of nanospecies that comprise non-spherical fairly compact domains, exhibiting an irregular surface.

The 250 nm Nanospecies Are Nanodroplets with Liquid-like Properties.

In an attempt to remove the scattering species from the solution, filtration through a 100 nm PTFE filter was carried out. Surprisingly multiple filtrations did not significantly change either the number or the size of the scattering species. The performance of the 100 nm PTFE filter was therefore tested using commercial solid polystyrene latex particle standards with diameters of 100 and 200 nm (see the Supporting Information). The 100 nm PTFE filters performed as expected and quantitatively removed both 200 and 100 nm solid nanoparticles from solution. Because the 250 nm scattering species present in the glycine solution were not removed by this same filtration process, they could clearly not be solid nanoparticles and were therefore identified as nanodroplets. The liquid-like properties of nanodroplets allow them to be squeezed through the nanopores of the hydrophobic PTFE filter and then reform again as 250 nm scattering species. It is noted that hydrophobic PTFE filters of this kind are commonly used to degas solutions, and so the nanospecies cannot be ascribed to nanobubbles, as is evidenced further below.

Interestingly, when filtration was carried out through a hydrophilic aluminum oxide filter (100 nm Anotop), it was found to be possible to lower the population of nanospecies in solution by an order of magnitude. Furthermore, when a finer 20 nm Anotop filter was used, the removal of nanodroplets was also accompanied by a clear increase in back-pressure. This observation suggests the nanodroplets bind strongly to the filter within the hydrophilic filter matrix, leading to a restriction of solvent flow through the pores.

It should be noted that mass spectrometry of solutions before and after filtration showed no significant change in the concentration of metal ions present, including aluminum (see the Supporting Information). HPLC also showed that the concentration of glycine in solution was unchanged following filtration through either type of filter (within the experimental error of the technique).

Nanodroplets Arise Directly from Dissolution of Glycine Crystals.

The rate of nucleation of glycine crystals from Anotop-filtered, quiescent solution was observed to be very slow with typically only a single crystal forming over several days. Aliquots of the mother liquor taken prior to the observation of any crystals consistently showed only very low levels of scattering nanospecies in the solution. Surprisingly, however, once a crystal had formed, gentle warming of the mother liquor to initiate partial dissolution quickly generated a much higher population of nanodroplets in the surrounding solution, as evidenced by both DLS and NTA. Figure 2 shows the DLS autocorrelation function obtained for a nanofiltered (20 nm Anotop) supersaturated solution prior to crystal growth and that obtained following partial redissolution of the formed glycine crystal on warming it in the mother liquor to 35 °C. For comparison, the data for pure water blank are also shown.

It can be seen that the scattering signal from the nanodroplets became much more evident in the nanofiltered solutions once crystals were also present. Significantly, a system containing saturated glycine solution, nanodroplets, and undissolved crystals was found to persist unchanged for weeks, suggesting an equilibrium position had been reached.

The DLS measurements also provided evidence for much smaller glycine molecular clusters in both the filtered and the unfiltered supersaturated solutions, with decay times of $\tau < 0.01$ ms (Figure 2). Similar cluster species were also observed in the

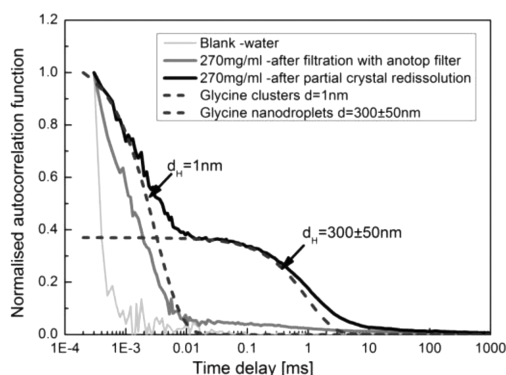


Figure 2. Normalized autocorrelation function ($g_2(\tau) - 1$) from DLS. Blank water (light gray), 270 mg/mL glycine solution after filtration (dark gray), and 270 mg/mL glycine solution after crystal formation and partial dissolution at 35 °C (black). Blank and solutions were initially filtered using a 20 nm Anotop filter and were measured at 25 °C. Dashed lines show separate theoretical autocorrelation functions for molecular clusters and nanodroplets.

SAXS measurements and exhibited an estimated radius of gyration (R_g) of around 0.25 nm (see the Supporting Information). From the fitting of the two separate decay parts of the DLS autocorrelation function, the average sizes of the smaller (first decay at smaller τ) and larger (second decay at larger τ) species were estimated using cumulant analysis.¹⁹ The mean hydrodynamic diameters of molecular clusters and nanodroplets were found to be 1 and 300 nm, respectively. The measured nanodroplet size from DLS was slightly greater than that observed by NTA, which is not unexpected: DLS provides an intensity weighted size average, which is sensitive toward small numbers of larger species, while nanoparticle tracking analysis (NTA) yields the number weighted size average.^{19,20}

The Scattering Species Are Glycine-Rich Nanodroplets. The appearance of nanodroplets in nanofiltered solutions only after the redissolution of glycine crystals provided good evidence that they contained glycine, but, to address the possibility they also contained a residual low level impurity, further purification experiments were undertaken. Repeated cycles of nanofiltration (20 nm Anotop filter) to remove nanodroplets, crystallization (via cooling), crystal isolation (via collection on a membrane filter), and glycine crystal redissolution (by warming) were undertaken. Following three successive cycles, the resultant solution was found to still contain nanodroplets of the same population and size. Because on each cycle most of the scattering species were removed prior to the crystallization step, it is highly unlikely that the nanodroplets reappearing each time could arise from adventitious impurities. If this were the case, the impurities would either be observable in solution, independent of whether glycine crystals had previously formed, or else they should be significantly reduced in number following each round of nanofiltration, crystallization, and dissolution. The possibility that the scattering species arose as a product of glycine reaction or breakdown within crystals was also discounted because of the very consistent number and size observed whatever the source, method, or time taken to prepare and redissolve crystals. It was concluded therefore that the scattering species could most reasonably be ascribed to formation of glycine-rich nanodroplets within bulk glycine saturated solution in equilibrium with glycine crystals.

The Time to Appearance of Glycine Crystals from Quiescent Solutions Is Independent of the Concentration of 250 nm Glycine-Rich Nanodroplets. The 250 nm glycine-rich nanodroplets would perhaps be expected to be intermediates on a two-step crystallization pathway. We therefore compared the time to appearance of crystals that had either been (a) freshly nanofiltered or (b) nanofiltered, crystallized by cooling, and then rewarmed to fully redissolve the crystals. In both cases, crystallization was carried out in glass vials containing supersaturated quiescent solution ($S = 1.1$), at 25 °C. Solutions prepared by method (a) contained around a 6-fold lower concentration of nanodroplets than about 10^9 per mL obtained with method (b). There was no detectable difference in the time to formation of visible crystals. Typically one or two crystals formed over a period of 30 ± 10 h and grew to several millimeters long.

Glycine Crystallization Is Significantly Faster in Solutions Stirred with a Magnetic Stirrer Bar. At the same low supersaturations used in the above study ($S = 1.1$), the time to formation of glycine crystals following continuous agitation of the solution with a magnetically driven stirrer bar was observed to be dramatically less. The effect was clear and highly reproducible, with a large number (hundreds to thousands) of crystals being formed in hours rather than a single (or few) crystal forming over several days. In these experiments, solutions were prepared and nanofiltered at 55 °C (20 nm Anotop) into a 7 mL glass vial (20 × 42 mm) and then cooled to 25 °C before being vigorously stirred using a pivot ring magnetic stirrer bar (12 × 6 mm). To eliminate potential effects of seeding by the bar, the average time to crystal formation was also measured with brand new bars in new vials and compared to the time with used carefully cleaned bars and vials; the results were the same.

Glycine Crystallization Is Unaffected by the Agitation of the Solution or the Presence of a Fixed Magnetic Stirrer Bar. To investigate the reason behind the observed accelerated crystallization, a more controlled experimental design was adopted. Supersaturated ($S = 1.1$) glycine solutions were prepared, nanofiltered (20 nm Anotop filter), and four different protocols applied (i) leaving the vial undisturbed, (ii) continuous inversion of the vial on a rotator, (iii) introduction of a fixed-in-place magnetic stirrer bar into the vial and continuous inversion on a rotator, and (iv) introduction of a free-to-tumble magnetic stirrer bar into the vial and continuous inversion on a rotator. The aim of the latter protocol was to ensure the stirrer bar would gently collide with the vial wall during each inversion. It was found that the average times required for formation of a clearly visible crystal (few mm long) using protocols (i), (ii), and (iii) were similar, being around 30 ± 10 h, and typically only a single large crystal was produced. These data from over 75 repeat experiments demonstrated that within experimental error nucleation was unaffected by the agitation arising from the continuous tumbling process. Hence, there was no observable effect of continuously changing the area of the air–water interface or introducing bubbles into the solution. Similarly, neither contact of the supersaturated glycine solution with the PTFE surface of the magnetic stirrer bar, nor the repeated flow over it during tumbling of the vial containing a fixed bar, had any measurable effect on the induction times.

Glycine Crystallization Is Accelerated by the Presence of a Tumbling Magnetic Stirrer Bar. When protocol (iv) was applied and the magnetic stirrer bar was allowed to gently collide with and slide along the vial wall, the time to formation

of many small, but easily observable, crystals was always very markedly reduced (80 experiments) and took around 3 ± 1.5 h. In these experiments, the solution typically remained optically clear for 2–3 h, whereupon at a certain point it suddenly became cloudy and a plethora of microcrystals started to grow rapidly. Many hundreds of needle-like crystals then became visible over a short time span (few minutes), and these then continued to grow for around 30 min, with many reaching a few hundreds of micrometers in length (Figure 3).

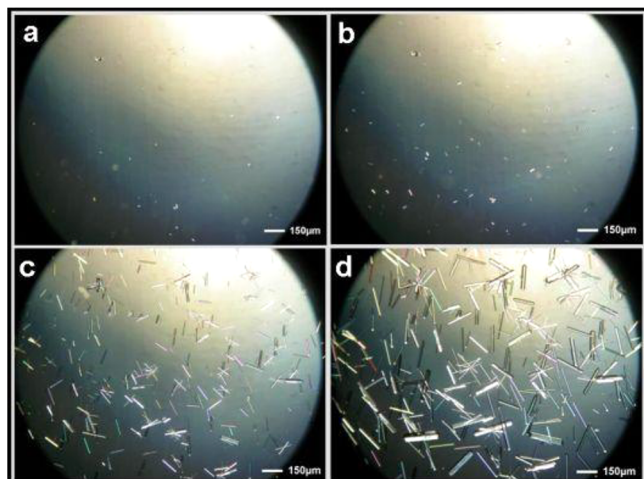


Figure 3. Photograph of crystals grown from 270 mg/mL glycine solution prepared in continuously inverted vial containing a tumbling stirrer bar (mixing time 3 h). Immediately on first detection of turbidity in the vial, an aliquot was placed on a microscope slide and covered to prevent evaporation. Images were taken after (a) 0 min, (b) 1 min, (c) 5 min, and (d) 10 min.

The Tumbling Magnetic Stirrer Bar Does Not Create Permanent New Nucleation Sites. To determine whether the acceleration effect was due solely to the mechanical action of the tumbling bar, protocol (iv) was applied to a filtered solution (20 nm Anotop), resulting in formation of microcrystals after about 3 h. This vial was tumbled further, overnight, whereupon the large crop of microcrystals was fully redissolved into the mother liquor by gentle heating. The same vial, unopened throughout, was then subjected to protocol (i), involving standing the supersaturated solution undisturbed at room temperature. The time to formation of a visible crystal was observed to revert to 30 ± 10 h as previously measured for (i). This experiment demonstrates that tumbling of the bar has no irreversible effect on the system and shows that that acceleration of crystallization is transient and not caused by tumbling-induced scratches or splinters to either the vial or the bar or else from production of other heterogeneous nucleation sites. Because the vial remained unopened throughout, any features generated on applying protocol (iv) would still be present when protocol (i) was subsequently applied, but nevertheless the time to formation of crystals was consistently 10 times longer.

Acceleration of Glycine Crystallization Is Not Due to Secondary Nucleation. It was postulated that the acceleration effect of the tumbling bar could perhaps arise from splintering of one or more nascent crystals leading to multiple secondary nucleation sites. To determine if this was a reasonable hypothesis, the growth rates of seed glycine crystals were measured in identical supersaturated solutions. The

measured initial growth rate for the crystals was determined to be $10 \pm 0.8 \mu\text{m}/\text{min}$. Such a rate means that were any nuclei to be produced within the first 2 h, they would grow in the undisturbed solution to be easily visible crystals (>2.5 mm) over the following 5–10 h. As detailed above, it was found that whenever the stationary crystallization protocol (i), or tumbling protocols (ii) and (iii), were applied, then no visible crystals were observed after 20 h. This would imply that in these solutions no nascent crystal could be present in the vial during at least the first 5 h. Because, invariably, when protocol (iv) was applied hundreds of rapidly growing microcrystals were observed within a time frame of less than 5 h, splintering of primary nascent crystal leading to secondary nucleation does not appear to be a tenable model. Powder X-ray diffraction showed that the microcrystals were of the same stable α -polymorph as large crystals formed in undisturbed solutions.

Accelerated Crystallization of Glycine Correlates with Production of Extremely Large Glycine-Rich Nanodroplets (>750 nm). Aliquots of solution were removed from vials that had been subjected to the different crystallization protocols, prior to formation of visible crystals, and analyzed by DLS and NTA. Aliquots from vials subjected to protocols (i), (ii), and (iii) showed only low levels of scattering nanospecies throughout. This is consistent with the removal of nanodroplets from solution by nanofiltration as observed previously. Surprisingly, aliquots from vials subjected to protocol (iv), even for a short time, were found to contain increased numbers of scattering nanodroplets. These were mainly of ~ 250 nm diameter, but there was also an additional population of much larger species, and as the vial was tumbled with the bar present, for longer, the numbers increased. Figure 4 shows the distribution of nanodroplets present after 1.5 h. At

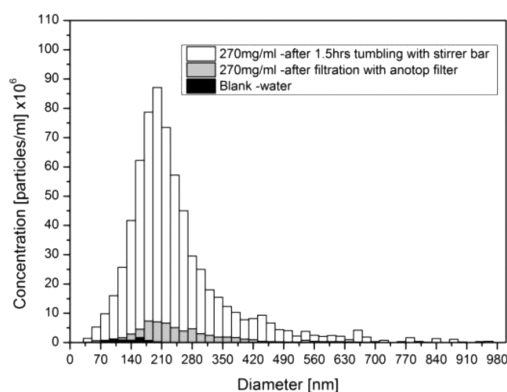


Figure 4. Nanodroplets size distribution (from NTA) at 25 °C. Blank water (black bars), 270 mg/mL glycine aqueous solution, after nanofiltration (light gray bars), and 270 mg/mL glycine aqueous solution, after 1.5 h tumbling with a magnetic stirrer bar (white bars). Blank and solutions were filtered using a 20 nm Anotop filter.

this time point, the population of nanodroplets of ~ 250 nm diameter was about twice that present in a quiescent PTFE filtered solution, but as shown earlier even a 6-fold change in the concentration of these species does not affect the nucleation kinetics. More notable was the significant increase in the concentration of much larger nanodroplets (see Figure 4). Thus, after 1.5 h the population of scattering species present with diameters greater than 500 and 750 nm was measured at 31×10^6 and 7.2×10^6 per mL, respectively. This compares to values of 1.9×10^6 and 0 per mL (not measurable) in the

starting nanofiltered solution. The generation of these extremely large nanodroplets (>750 nm) appears to be induced by the gentle collision of the stirrer bar with the vial wall and may well arise from coalescence of smaller surface-attached nanodroplets. Control experiments showed that if the same protocol (iv) was repeated with a vial of pure water, even for several days, no new scattering species were observed by NTA, ruling out glass fragments as a source of particles. Because the accelerated crystallization process can only be induced by introduction of the tumbling bar and this uniquely leads to the formation of extremely large nanodroplets, it is reasonable to propose the two phenomena are correlated.

DISCUSSION

There have been a number of studies aimed at identifying potential prenucleation species in glycine solutions.^{2,3,5} In general, these have only used techniques sensitive to very small (subnanometer) clusters. However, it has been suggested previously that larger metastable liquid-like clusters may be transiently formed from these smaller subnanometer clusters in supersaturated solutions and that these could then undergo reorganization into crystalline nuclei.⁵ In this work, we used a range of complementary scattering techniques capable of detecting both very small molecular clusters and much larger nanodroplets. We also designed experiments capable of monitoring species in equilibrium with crystals.

An early key finding was that in just-saturated aqueous glycine solutions and in solutions containing excess glycine crystals, both molecular clusters and very large nanospecies (250 nm) coexisted (Figure 1a). Furthermore, they remained indefinitely at the same relative concentration, suggesting this may be an equilibrium position. The larger species were shown to be nanodroplets that could be passed unchanged through a 100 nm hydrophobic filter (PTFE) but completely removed from solution by nanofiltration using a 100 or 20 nm hydrophilic filter (Anotop). The smaller molecular clusters were unaffected by nanofiltration through either PTFE or Anotop filters and exhibited SAXS behavior identical to that previously reported for glycine solutions (Figure 1b). Interestingly, it was found that the SAXS data for the larger scattering nanospecies could not be fitted using a model based on spheres with sharp interfaces. This, combined with the persistence of the species on filtration through a PTFE filter, ruled out nanobubbles as the source of the scattering. A more sophisticated analysis of the SAXS data indicated that it could be fitted very well with a model based on nanospecies comprising fairly compact clusters with a highly irregular surface (Figure 1b). The presence of an irregular surface is unusual and would suggest a very low interfacial energy, perhaps arising from a similarity in composition between the nanospecies and the bulk solution leading to undulating interfacial topology similar to complex surfactant or block-copolymer systems.

The ability to significantly reduce the concentration of the larger scattering nanospecies by nanofiltration proved to be a very important experimental tool because it enabled effective discrimination to be carried out between impurities and glycine containing species. It was found that within a stationary nanofiltered saturated glycine solution, only very low levels of nanodroplets were observed over tens of hours. However, as soon as crystals formed from the solution, the concentration of 250 nm nanodroplets rose by around an order of magnitude (Figure 2). Multiple cycles of nanofiltration and crystallization

did not change the way the system behaved, and concomitant with glycine crystal formation, nanodroplets of a similar size and at a similar concentration consistently reappeared. It was therefore concluded that the nanospecies could not be impurities but must arise directly from dissolution of glycine crystals. The scattering species were therefore identified as glycine-rich nanodroplets.

It was surprising to discover that such large glycine-rich molecular assemblies were stable within just-saturated aqueous solutions. However, there is a clear kinetic barrier to their formation because in nanofiltered solutions they only increase in concentration rapidly once crystals have formed. It seems probable that they are preferentially formed by a mechanism involving solvent-mediated partial breakdown of glycine crystals. Thus, penetration of solvent into an outer crystal lattice may lead to spaying off of nanoscale domains, which subsequently become partially solvated to produce glycine-rich nanodroplets. One intriguing possibility is that these nanodroplets may have a composition/structure similar to that of lyotropic liquid crystals.

It would clearly be of significant interest to directly determine the composition of the nanodroplets. From the estimated population of 10^9 per mL, and the measured diameter of 250 nm, it was calculated that the maximum mole fraction of glycine that could be physically contained within the nanodroplets must be less than 10^{-6} . This corresponds to an upper total concentration of $<0.3 \mu\text{g/mL}$ dispersed within 270 mg/mL of molecularly dissolved glycine. The large background signal arising from dissolved glycine means that determining the composition of the nanodroplets is an extremely challenging analytical problem, and as yet no method has been identified. The extremely low mole fraction of glycine in the nanodroplets is of course consistent with not being able to detect differences in glycine concentration, following nanofiltration. It also explains why the equilibrium with crystals can be repeatedly re-established.

Two-step nucleation processes involving intermediate solute-rich nanodroplets have been proposed in a number of crystallizing systems. It was therefore of interest to try and determine if the 250 nm nanodroplets played a role in the nucleation of glycine crystals. In fact, it was found that the time to formation of visible crystals from quiescent supersaturated glycine solutions containing 10^9 per mL nanodroplets, or else 6-fold lower concentrations, was indistinguishable. In both cases, only one or two individual crystals formed after a period of 30 ± 10 h. This would suggest that the observed 250 nm glycine-rich nanodroplets play no direct role in promoting nucleation of viable crystals.

An interesting discovery was made when glycine solutions of supersturation ($S = 1.1$) identical to that used in the above quiescent experiment were rapidly stirred using a magnetic stirrer bar; a plethora of microcrystals would suddenly and consistently appear after 2–3 h stirring (Figure 3). A series of carefully designed experiments were used to identify the cause of this unexpected acceleration of the glycine crystallization process. These were able to systematically eliminate many of the possible factors including transient changes to the solvent–air interface including bubble formation; the presence in the system of the PTFE surface of the stirrer bar; flow of the supersaturated solution over the vial bar surfaces; and production of new heterogeneous nucleation sites caused by gentle collision of the bar with the vial wall and secondary nucleation from previously formed glycine crystals. The key

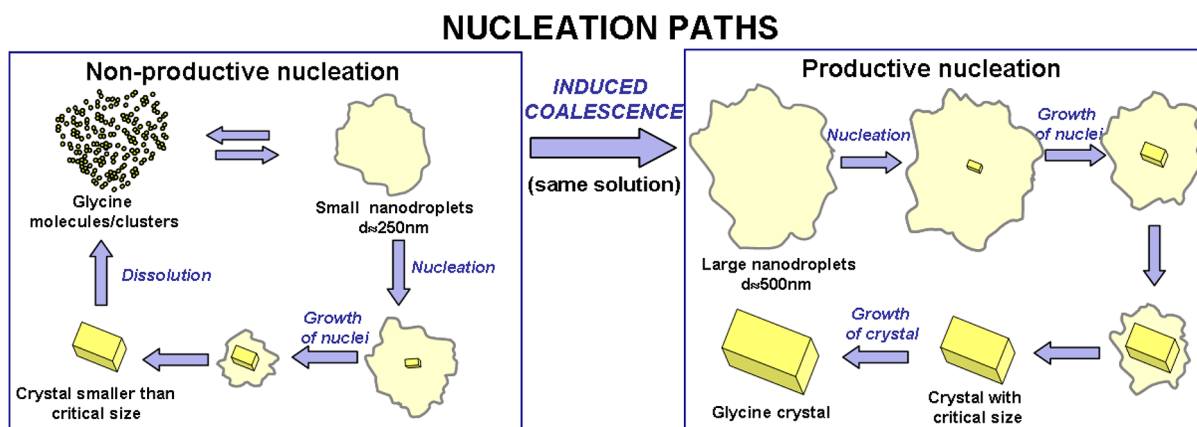


Figure 5. Effect of nanodroplet size on the outcome of nucleation.

factor remaining was an absolute requirement for the stirrer bar to be free to tumble and collide with the vial wall during the 2–3 h incubation period prior to microcrystal formation. It was further established that this gentle collision process leads to a dramatic increase in the number of scattering nanodroplets in the solution. The majority of these were in the 250 nm size range shown previously to play no part in promoting rapid crystal formation. However, the tumbling bar process also generated a subpopulation of extremely large nanodroplets (>750 nm). These reached a concentration of more than 10^6 per mL in the tumbled solutions while being undetectable in quiescent solutions. It is proposed therefore that these extremely large glycine-rich nanodroplets must be key to the rapid crystallization process.

In the following section, we provide a model that attempts to rationalize this complete data set. First, the scattering data demonstrate that saturated aqueous solutions of glycine invariably have a very low mole fraction of solute contained within glycine-rich nanodroplets. These nanodroplets are not metastable and exist at a fixed concentration in equilibrium with glycine crystals. In fact, even below the saturation concentration, a lower population of nanodroplets remains (unpublished data). On dissolution of crystals, nanodroplets are able to form facily because of the high local glycine concentration at the crystal surface. However, in nanofiltered saturated solutions (20 nm Anotop filter) in which a large proportion of the nanodroplets have been removed, a kinetic barrier exists that attenuates re-establishment of the solution equilibrium speciation. It is proposed that this is because if crystals are not present the nanodroplets preferentially reform on the vial walls. Here, they remain loosely adhered and so cannot be observed by scattering measurements. The existence of this large, loosely bound, surface population is clearly demonstrated by the experiments with the tumbling stirrer bar. The low intensity mechanical action, provided by the gentle collision of the small stirrer bar with the vial wall, is sufficient to displace nanodroplets back into solution. In the absence of this mechanical process, no change in the solution concentration is observed over tens of hours. Crucially, an additional effect of the repeated gentle collision process is to induce coalescence within a small proportion of the surface bound nanodroplets. This results in the formation of a subpopulation of much larger glycine-rich nanodroplets (>750 nm) that are never observed under equilibrium conditions. These are likely to have a composition similar to that of the smaller 250 nm nanodroplets but will contain a much larger total mass of glycine.

The presence of these extremely large glycine-rich nanodroplets, at a concentration of $\sim 10^6$ per mL, coincides with the onset of a significantly accelerated crystallization process for glycine. Thousands of microcrystals are observed to form in 3–5 hours rather than the one or two large crystals that are usually produced after tens of hours. This can be rationalized by proposing that, first, nucleation is much faster within glycine-rich nanodroplets than in the more dilute bulk solution, and, second, productive nucleation requires nanodroplets large enough to contain a critical mass of glycine. In this model, it is proposed that each time nucleation is initiated within a solute-rich nanodroplet, crystal growth will proceed rapidly until the local high concentration of glycine is exhausted whereupon the nascent crystal will become exposed to the surrounding molecular solution of glycine: if at this point the crystal is large enough, it will survive and grow; otherwise, it will necessarily redissolve back into the bulk. Within quiescent solutions, coalescence events and productive nucleation appear to be very rare and most likely occur at the vial wall. On the other hand, the mechanical action of the tumbling stirrer bar is able to generate millions of coalesced nanodroplets above the critical size and leads to productive nucleation of thousands of crystals. Figure 5 illustrates this model of productive and nonproductive nucleation from solute-rich nanodroplets. In the system under study, the equilibrium population of 250 nm glycine-rich nanodroplets undergoes exclusively nonproductive nucleation because they are below the critical size (Figure 5, left panel). This explains why even when there are 10^9 per mL of nanodroplets at $S = 1.1$, only single crystals form. On the other hand, mechanically coalesced glycine-rich nanodroplets present at 10^6 per mL but with a diameter of >750 nm lead to efficient productive nucleation of crystals because they are above the critical size (Figure 5, right panel).

The above identified pathway of nucleation within nanodroplets is superficially similar to the two-step nucleation process previously put forward for proteins and small molecules.^{2,5,7–10,16,17,21–24} However, it differs significantly in that it identifies that the solute-rich molecular assemblies relevant to crystallization are much larger (>750 nm) than those discussed or proposed in earlier studies. Furthermore, the very small molecular assemblies that were identified previously (up to 1–2 nm) as being important did not change in size or population throughout the crystallization process. It is probable that solute molecules will continuously redistribute between molecular solution, small molecular clusters, and nanodroplets. Because the nanodroplets are not isolable and are estimated to

only contain 10^{-6} mole fraction of the total solute, it would be extremely difficult to resolve a specific spectroscopic signal for them, and this could explain why they have not been identified in the other studies.

It is recognized that in addition to inducing coalescence, the collision of the stirrer bar with surface bound nanodroplets could also potentially induce a direct mechanical alignment process, of the kind observed for liquid crystals, which could potentially also contribute to the observed accelerated crystallization process. However, because of the fast growth rate for glycine crystals, it might be expected that an alignment process would result in only a relatively small number of nucleated crystals, not the many thousands observed.

Considering crystallization more generally, it is interesting to note that the age-old practice of rubbing (or “scratching”) the inner surface of a crystallization vessel is very similar to the mechanical effect of the stirrer bar protocol that was applied in this study. Even without scratching, rubbing would tend to coalesce unseen surface-bound nanodroplets, and this may explain why this simple technique appears to provide a general way of accelerating crystal formation. Conversely, functionalized surfaces designed to promote rapid nucleation may actually lead to elimination of smaller nanodroplets before they are able to reach a critical size confounding this type of approach.

CONCLUSION

These data show that the dissolution of glycine crystals into water to form a saturated solution invariably leads to formation of a population of around 10^9 per mL of glycine-rich nanodroplets with mean diameter of around 250 nm. These species are very stable and exist within glycine aqueous solution in equilibrium with glycine crystals. Similar sized nanodroplets are observed in supersaturated solutions but do not appear to play a productive role in the nucleation of glycine crystals. The stirrer bar-induced coalescence of surface bound glycine rich nanodroplet in supersaturated solution generated a small population of 10^6 per mL of much larger nanodroplets (>750 nm). The presence of these species correlated with a significant acceleration in the rate of glycine crystal formation. It is therefore concluded that at moderate glycine supersaturation, extremely large glycine-rich nanodroplets are required to provide the critical mass of glycine required for productive nucleation.

ASSOCIATED CONTENT

Supporting Information

Additional experimental details. This material is available free of charge via the Internet at <http://pubs.acs.org>.

AUTHOR INFORMATION

Corresponding Author

*Tel.: +44 (0) 141 548 2301. Fax: +44 (0) 141 548 4822. E-mail: b.d.moore@strath.ac.uk.

Notes

The authors declare no competing financial interest.

ACKNOWLEDGMENTS

This project was supported by the BBSRC Bioprocessing Research Industry Club, Grant Reference BB/F004664/1, and by the Synchrotron SOLEIL (proposal 20100344). We would

like to thank Dr. Javier Perez for his assistance with measurements and data analysis.

REFERENCES

- (1) Parveen, S.; Davey, R. J.; Dent, G.; Pritchard, R. G. Linking solution chemistry to crystal nucleation: the case of tetrolic acid. *Chem. Commun.* **2005**, *12*, 1531–1533.
- (2) Erdemir, D.; Chattopadhyay, S.; Guo, L.; Ilavsky, J.; Amenitsch, H.; Segre, C. U.; Myerson, A. S. Relationship between self-association of glycine molecules in supersaturated solutions and solid state outcome. *Phys. Rev. Lett.* **2007**, *99*, 115702.
- (3) Hamad, S.; Hughes, C. E.; Catlow, C. R. A.; Harris, K. D. M. Clustering of glycine molecules in aqueous solution studied by molecular dynamics simulation. *J. Phys. Chem. B* **2008**, *112*, 7280–7288.
- (4) Chiarella, R. A.; Gillon, A. L.; Burton, R. C.; Davey, R. J.; Sadiq, G.; Auffret, A.; Cioffi, M.; Hunter, C. A. The nucleation of inosine: the impact of solution chemistry on the appearance of polymorphic and hydrated crystal forms. *Faraday Discuss.* **2007**, *136*, 179–193.
- (5) Chattopadhyay, S.; Erdemir, D.; Evans, J. M. B.; Ilavsky, J.; Amenitsch, H.; Segre, C. U.; Myerson, A. S. SAXS study of the nucleation of glycine crystals from a supersaturated solution. *Cryst. Growth Des.* **2005**, *5*, 523–527.
- (6) Meldrum, F. C.; Sear, R. P. Now you see them. *Science* **2008**, *322*, 1802–1803.
- (7) Vekilov, P. G. Metastable mesoscopic phases in concentrated protein solutions. *Ann. N.Y. Acad. Sci.* **2009**, *1161*, 377–386.
- (8) Lutsko, J. F.; Nicolis, G. Theoretical evidence for a dense fluid precursor to crystallization. *Phys. Rev. Lett.* **2006**, *96*, 046102.
- (9) Gliko, O.; Pan, W.; Katsonis, P.; Neumaier, N.; Galkin, O.; Weinkauf, S.; Vekilov, P. G. Metastable liquid clusters in super- and undersaturated protein solutions. *J. Phys. Chem. B* **2007**, *111*, 3106–3114.
- (10) Wolde, P. R. t.; Frenkel, D. Enhancement of protein crystal nucleation by critical density fluctuations. *Science* **1997**, *277*, 1975–1978.
- (11) Xu, A.-W.; Ma, Y.; Colfen, H. Biomimetic mineralization. *J. Mater. Chem.* **2007**, *17*, 415–449.
- (12) Bonnett, P. E.; Carpenter, K. J.; Dawson, S.; Davey, R. J. Solution crystallisation via a submerged liquid-liquid phase boundary: oiling out. *Chem. Commun.* **2003**, *6*, 698–699.
- (13) Stephens, C. J.; Kim, Y.-Y.; Evans, S. D.; Meldrum, F. C.; Christenson, H. K. Early stages of crystallization of calcium carbonate revealed in picoliter droplets. *J. Am. Chem. Soc.* **2011**, *133*, 5210–5213.
- (14) Ma, Y.; Cölfen, H.; Antonietti, M. Morphosynthesis of alanine mesocrystals by pH control. *J. Phys. Chem. B* **2006**, *110*, 10822–10828.
- (15) Niederberger, M.; Colfen, H. Oriented attachment and mesocrystals: Non-classical crystallization mechanisms based on nanoparticle assembly. *Phys. Chem. Chem. Phys.* **2006**, *8*, 3271–3287.
- (16) Cölfen, H.; Mann, S. Higher-order organization by mesoscale self-assembly and transformation of hybrid nanostructures. *Angew. Chem., Int. Ed.* **2003**, *42*, 2350–2365.
- (17) Schwahn, D.; Ma, Y.; Cölfen, H. Mesocrystal to single crystal transformation of D,L-alanine evidenced by small angle neutron scattering. *J. Phys. Chem. C* **2007**, *111*, 3224–3227.
- (18) Linder, P.; Zember, T.; Pusey, P. N. *Neutron, X-rays and Light Scattering Methods to Soft Condensed Matter. Introduction to Scattering Experiments*; Elsevier Science B.V.: New York, 2002.
- (19) Finsy, R. Particle sizing by quasi-elastic light scattering. *Adv. Colloid Interface Sci.* **1994**, *52*, 79–143.
- (20) Gallego-Urrea, J. A.; Tuoriniemi, J.; Hassellöv, M. Applications of particle-tracking analysis to the determination of size distributions and concentrations of nanoparticles in environmental, biological and food samples. *Trends Anal. Chem.* **2011**, *30*, 473–483.
- (21) Kashchiev, D.; Vekilov, P. G.; Kolomeisky, A. B. Kinetics of two-step nucleation of crystals. *J. Chem. Phys.* **2005**, *122*, 244706.
- (22) Yau, S. T.; Vekilov, P. G. Quasi-planar nucleus structure in apoferritin crystallization. *Nature* **2000**, *406*, 494–497.

- (23) Erdemir, D.; Lee, A. Y.; Myerson, A. S. Nucleation of crystals from solution: Classical and two-step models. *Acc. Chem. Res.* **2009**, *42*, 621–629.
- (24) Vekilov, P. G. Nucleation. *Cryst. Growth Des.* **2010**, *10*, 5007–5019.